DNA Modifications by a Novel Bifunctional Trinuclear Platinum Phase I Anticancer Agent†

Viktor Brabec,‡ Jana Kašpárková,‡ Oldøich Vrána,‡ Olga Nováková,‡ John W. Cox,§ Yun Qu,§ and Nicholas Farrell*,§

Institute of Biophysics, Academy of Sciences of the Czech Republic, CZ-61265 Brno, Czech Republic, and Department of Chemistry, Virginia Commonwealth University, Richmond, VA 23284-2006

Received January 20, 1999

ABSTRACT: The DNA-binding profile of a novel, trinuclear platinum Phase I clinical agent (BBR3464) is summarized. The structure of BBR3464 is best described as two *trans*-[$PtCl(NH_3)_2$] units linked by a tetra-amine [*trans*-$Pt(NH_3)_2\{H_2N(CH_2)_6NH_2\}_2]^{2+}$ unit. The +4 charge of BBR3464, the presence of at least two Pt coordination units capable of binding to DNA, and the consequences of such DNA binding are remarkable departures from the cisplatin structural paradigm. The chemical and biological features argue that the drug should be considered the first clinical representative of an entirely new structural class of DNA-modifying anticancer agents. The high charge on BBR3464 facilitates rapid binding to DNA with a $t_{1/2}$ of ∼40 min, significantly faster than the neutral cisplatin. The melting temperature of DNA adducted by BBR3464 increased at low ionic strength but decreased in high salt for the same r_b. This unusual behavior is in contrast to that of cisplatin. BBR3464 produces an unwinding angle of 14° in negatively supercoiled pSP73 plasmid DNA, indicative of bifunctional DNA binding. Quantitation of interstrand DNA−DNA cross-linking in plasmid pSP73 DNA linearized by *Eco*RI indicated approximately 20% of the DNA to be interstrand cross-linked. While this is significantly higher than the value for cisplatin, it is, interestingly, lower than that for dinuclear platinum compounds such as [{*trans*-$PtCl(NH_3)_2\}_2H_2N(CH_2)_6$-$NH_2]^{2+}$ (BBR3005) where interstrand cross-linking efficiency may be as high as 70−90%. Either the presence of charge in the linker backbone or the increased distance between platinating moieties may contribute to this relatively decreased ability of BBR3464 to induce DNA interstrand cross-linking. Fluorescence experiments with ethidium bromide were consistent with the formation of long-range delocalized lesions on DNA produced by BBR3464. The sequence preference for BBR3464 on plasmid DNA was determined to the exact base pair by assaying extension of the polynucleotide by $Vent_R(exo^+)$ DNA polymerase. Strong sequence preference for single dG or d(GG) sites was suggested. The presence of relatively few blocks on DNA in comparison to either cisplatin or BBR3005 was indicative of high sequence selectivity. The following appropriate sequence where stop sites occur was chosen:

5′– $T'_{23}\,G'_{24}\,A'_{25}\,A'_{26}\,T'_{27}\,T'_{28}\,C'_{29}\,G'_{30}\,A'_{31}\,G'_{32}\,C'_{33}\,T'_{34}\,C'_{35}\,G'_{36}\,G'_{37}\,T'_{38}\,A'_{39}$

3′– $A_{23}\,C_{24}\,T_{25}\,T_{26}\,A_{27}\,A_{28}\,G_{29}\,C_{30}\,T_{31}\,C_{32}\,G_{33}\,A_{34}\,G_{35}\,C_{36}\,C_{37}\,A_{38}\,T_{39}$

molecular modeling on 1,4 interstrand (G'_{30} to G_{33}) and 1,5 intrastrand (G_{33} to G_{29}) cross-links further confirmed the similarity in energy between the two forms of cross-link. Finally, immunochemical analysis confirmed the unique nature of the DNA adducts formed by BBR3464. This analysis showed that antibodies raised to cisplatin-adducted DNA did not recognize DNA modified by BBR3464. In contrast, DNA modified by BBR3464 inhibited the binding of antibodies raised to transplatin-adducted DNA. Thus, the bifunctional binding of BBR3464 contains few similarities to that of cisplatin but may have a subset of adducts recognized as being similar to the transplatinum species. In summary, the results point to a unique profile of DNA binding for BBR3464, strengthening the originial hypothesis that modification of DNA binding in manners distinct from that of cisplatin will also lead to a distinct and unique profile of antitumor activity.

Dinuclear and trinuclear platinum complexes represent a new class of anticancer agents, distinct in DNA binding and antitumor activity from their mononuclear counterparts. The utility of the dinuclear motif in drug design was first demonstrated by linking two antitumor active cisplatin[1] {i.e., *cis*-$[PtCl_2(NH_3)]$, *cis*-DDP} units by a flexible diamine chain (*1*). Incorporation of the cisplatin synthon into linear trinuclear systems was also achieved (*2*). Chemical studies since then have shown that dinuclear and trinuclear com-

† The authors acknowledge support of this work by National Institutes of Health (RO1-CA78754), National Science Foundation (INT-9805552 and CHE-9615727), American Cancer Society (RPG89-002-11-CDD), Roche-Boehringer Mannheim, the Grant Agency of the Czech Republic (Grants No. 305/99/065, 307/97/P029, and 204/97/P028), and Grant Agency of the Academy of Sciences of the Czech Republic (Grants No. A5004702 and A7004805). The research of V.B. was also supported by an International Research Scholar's award from the Howard Hughes Medical Institute.

‡ Academy of Sciences of the Czech Republic.
§ Virginia Commonwealth University.

10.1021/bi990124s CCC: $18.00
Published on Web 05/06/1999

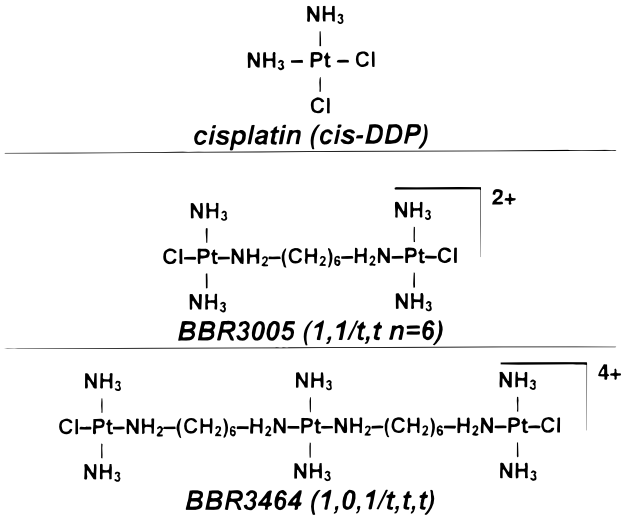

FIGURE 1: Structures of cisplatin, a representative dinuclear platinum compound (BBR3005), and the clinical drug BBR3464. In agreement with our previously used abbreviation system (*5*), BBR3464 would be 1,0,1/t,t,t indicating an all trans configuration and one Cl on the two terminal Pt atoms. For consistency with other citations describing the chemistry and biology of this new drug (see text), the BBR numbers will be used throughout.

pounds represent a large and diverse class of structures which may be differentiated among themselves with respect to important parameters of biological activity (*3*). Of special interest was the demonstration that compounds such as $[\{trans\text{-}PtCl(NH_3)_2\}_2H_2N(CH_2)_nNH_2]^{2+}$ (1,1/t,t, Figure 1) display cytotoxicity and antitumor activity in their own right and especially retained activity in cell lines resistant to cisplatin (*4*). Thus, the linking of two mononuclear, monofunctional *antitumor inactive* moieties produces formally bifunctional DNA binding agents. In this manner, chemical and biological comparisons with the classical mononuclear *cis*- and *trans*-$[PtCl_2(NH_3)_2]$ could be made (*5*). Geometric isomers exist in dinuclear chemistry because the Cl ligand can be *cis* or *trans* to the diamine bridge. Antitumor activity of bifunctional dinuclear and trinuclear platinum complexes is affected by nature of the coordination sphere, chain length, and steric effects within the linker group (*6*).

The first representative of this class, presently denoted BBR3464, entered Phase I clinical trials in June 1998. Its structure is best described as two *trans*-$[PtCl(NH_3)_2]$ units linked by a tetra-amine $[trans\text{-}Pt(NH_3)_2\{H_2N(CH_2)_6NH_2\}_2]^{2+}$ unit (1,0,1/t,t,t, Figure 1). This structure is a further step removed from the classical structure−activity relationships of platinum compounds and arose from systematic drug development efforts. The central unit does not contribute to covalent DNA binding but incorporates into the linker backbone a charge and hydrogen-bonding capacity which dramatically increase the DNA affinity, affect the charge/lipophilicity balance, and further increase the distance between the two Pt-DNA-binding coordination spheres. The choice of BBR3464 was made because of its dramatically enhanced antitumor efficacy in comparison to that of cisplatin and, indeed, "simple" dinuclear platinum compounds as represented by BBR3005 (Figure 1). Specifically, BBR3464 is cytotoxic at a 10-fold *lower* concentration than cisplatin and retains activity in cisplatin-resistant cell lines. Importantly, BBR3464 also displays consistently high antitumor activity in human tumor xenografts characterized as mutant p53 (ref *7* and Pratesi et al., unpublished results). This important feature suggests that the new agent may find utility in the over 60% of cancer cases where mutant p53 status has been indicated. DNA damage by chemotherapeutic agents is in many cases mediated through the p53 pathway (*8*). Consistently, cytotoxicity displayed in mutant cell lines would suggest an ability to bypass this pathway (Pratesi et al., unpublished results). As such, understanding the patterns of DNA damage which may lead to differential cell signaling is essential. The +4 charge of BBR3464, the presence of at least two Pt coordination units capable of binding to DNA, and the consequences of such DNA binding are remarkable departures from the cisplatin structural paradigm. The chemical and biological features argue that the drug should be considered the first representative of an entirely new structural class of DNA-modifying anticancer agents. With this advance the paradigm of cisplatin-based antitumor agents is altered.

This paper reports on the DNA-binding profile of BBR3464 and its relationship to the remarkable potency and antitumor activity of the new drug. Two major questions are how the profile differs with respect to cisplatin and the dinuclear analogue BBR3005. In this manner, we can distinguish the general class of lesions that distinguish BBR3464 from the mononuclear compound. Trinuclear and dinuclear bifunctional DNA-binding agents share many common structural features. The obvious differences which may account for the enhanced antitumor activity of BBR3464 and dinuclear-polyamine-linked compounds are the extended distance between platinating sites and the presence of charge along the backbone. Comparison of DNA-binding profiles may help to further delineate the critical structural features responsible for the biological activity of these new agents. In this way, we aim to place the DNA-binding profile in context, not only with cisplatin but also with other clinically used DNA-binding agents.

MATERIALS AND METHODS

Starting Materials. Cisplatin, *trans*-diamminedichloroplatinum(II) (transplatin), and chlorodiethylenetriamineplatinum(II) chloride, [PtCl(dien)]Cl, were synthesized and characterized in Lachema a.s. (Brno, Czech Republic). The dinuclear complex BBR3005 was prepared and characterized as described previously (*9*). The trinuclear complex BBR3464 was a gift from Ernesto Menta of Roche-Boehringer Mannheim. The stock solutions of the platinum complexes (5×10^{-4} M in 10 mM $NaClO_4$) were prepared in the dark at 25 °C and stored for at least 7 days before they were used. Calf thymus DNA (42% G + C, mean molecular mass ca. 2×10^7) was also prepared and characterized as described previously (*10*, *11*). Plasmid pSP73 (2464 bp) was isolated according to standard procedures and banded twice in CsCl/EtBr equilibrium density gradients. Restriction endonucleases

[1] Abbreviations: cisplatin, *cis*-diamminedichloroplatinum(II); DPP, differential pulse polarography; ELISA, enzyme-linked immunosorbent assay; EtBr, ethidium bromide; FAAS, flameless atomic absorption spectrophotometry; [PtCl(dien)]Cl, chlorodiethylenetriamineplatinum(II) chloride; r_b, the number of the molecules of platinum complex coordinated per nucleotide residue; r_i, the molar ratio of free platinum complex to nucleotide phosphates at the onset of incubation with DNA; $t_{1/2}$, half-time; t_m, DNA melting temperature; transplatin, *trans*-diamminedichloroplatinum(II).

and Thermal Cycle Dideoxy DNA sequencing kit with $Vent_R(exo^-)$ or $Vent_R(exo^+)$ DNA polymerases were purchased from New England Biolabs (Beverly, MA). A primer 5′-d(GATTTAGGTGACACTATAG) was from BioVendor (Brno, Czech Republic). EtBr, acrylamide, (bis)acrylamide, and urea were from Merck KgaA (Darmstadt, Germany). The radioactive products were from Amersham (Arlington Heights, IL).

Platination Reactions. Calf thymus and plasmid DNAs were incubated with platinum complex in 10 mM $NaClO_4$ at 37 °C for 48 h in the dark. The number of molecules of the platinum compound bound per nucleotide residue (r_b values) was determined by flameless atomic absorption spectrophotometry (FAAS) or by differential pulse polarography (DPP) (*12*).

DNA Melting. The melting curves of DNAs were recorded by measuring the absorbance at 260 nm. The melting curves of unplatinated or platinated DNA were recorded after Tris-HCl/EDTA buffer and $NaClO_4$ were added so that the resulting media contained 0.01−0.2 M $NaClO_4$ with 1 mM Tris-HCl/0.1 mM EDTA, pH 7.4. The value of the melting temperature (t_m) was determined as the temperature corresponding to a maximum on the first-derivation profile of the melting curves. The t_m values could be thus determined with an accuracy of ±0.3 °C.

Fluorescence Measurements. These measurements were performed on a Shimadzu RF 40 spectrofluorophotometer using a 1 cm quartz cell. Fluorescence measurements of DNA modified by platinum in the presence of EtBr were performed at an excitation wavelength of 546 nm, and the emitted fluorescence was analyzed at 590 nm. The fluorescence intensity was measured at 25 °C in 0.4 M NaCl to avoid secondary binding of EtBr to DNA (*13*, *14*). The concentrations were 0.01 mg/mL for DNA and 0.04 mg/mL for EtBr, which corresponded to the saturation of all intercalation sites of EtBr in DNA (*13*).

DNA Interstrand Cross-Link Assay. BBR3464 at varying concentrations was incubated with 2 μg of pSP73 DNA linearized by *Eco*RI. The platinated samples were precipitated by ethanol and analyzed for DNA interstrand cross-links in the same way as described in several recent papers (*4*, *15*). The linear duplexes were first 3′-end-labeled by means of Klenow fragment of DNA polymerase I in the presence of [α-^{32}P]dATP. The samples were deproteinized by phenol and precipitated by ethanol, and the pellet was dissolved in 18 μL of a solution containing 30 mM NaOH, 1 mM EDTA, 6.6% sucrose, and 0.04% bromophenol blue. The amount of interstrand cross-links was analyzed by electrophoresis under denaturing conditions on alkaline agarose gel (1%). After the electrophoresis was completed, the intensities of the bands corresponding to single strands of DNA and interstrand cross-linked duplex were quantified by means of a Molecular dynamics phosphorimager (Storm 860 system with ImageQuant software).

Unwinding of Negatively Supercoiled DNA. Unwinding of closed circular supercoiled pSP73 plasmid DNA was assayed by an agarose gel mobility shift assay (*16*). The unwinding angle Φ induced per platinum−DNA adduct was calculated upon the determination of the r_b value at which the complete transformation of the supercoiled to relaxed form of the plasmid was attained. Samples of pSP73 plasmid were incubated with BBR3464 at 37 °C in the dark for 48 h. All samples were precipitated by ethanol and redissolved in the TBE (Tris-borate/EDTA) buffer. An aliquot of the precipitated sample was subjected to electrophoresis on 1% agarose gels running at 25 °C in the dark with TBE buffer and the voltage set at 30 V. The gels were then stained with EtBr, followed by photography on Polaroid 667 film with transilluminator. The other aliquot was used for the determination of r_b values by FAAS.

Sequence Specificity of DNA Adducts. The fragment of pSP73 DNA linearized by *Nde*I (*Nde*I cuts only once within this plasmid) was obtained as previously described (*15*, *17*). Ten micrograms of pSP73 was treated with *Nde*I to obtain linear plasmid. After deproteinization by phenol/chloroform the modification of this fragment by BBR3005 (1,1/t,t) or BBR3464 (1,0,1/t,t,t) was carried out in 10 mM $NaClO_4$ for 48 h at 37 °C to obtain $r_b = 0.005$. CircumVent Thermal Cycle Dideoxy DNA sequencing kit with $Vent_R(exo^-)$ or (exo^+) DNA polymerases was used along with the protocol for thermal cycle DNA sequencing with 5′-end-labeled primer recommended by the manufacturer with small modifications (*18*).

Molecular Modeling. To correlate with the DNA cross-linking results, the fragment 5′-d(TGAATTCGAGCTCGGTA)/5′-d(TACCGAGCTCGAATTCA) (17 base pairs) was chosen, beginning with $T'_{23}\cdot A_{23}$ base pair of the overall sequence of pSP73 DNA (the relevant portion of which is shown in Figure 7B). The computations were performed using the program HyperChem (HyperCube, Inc., Ontario, Canada; Molecular Simulations, Inc., San Diego, CA.) on a Pentium PC with the AMBER parameter set and all-atom force field DNA/Pt, developed by Yao, et al. (*19*). The distance-dependent dielectric constant of $\epsilon = 4r_{ij}$ commonly used for calculations of DNA was applied to account for solvent effects (*20*). Counterions of charge +1.00 from the program's database were included at a distance of 0.167 nm from the phosphate oxygens of each base. The electrostatic and van der Waals terms were each scaled by 0.5, which is also common practice for calculations involving DNA. The models are constructed using the nucleic acids database to construct B-form DNA of the desired sequence and the builder module to construct BBR3464. Once the DNA is constructed, $-Pt(NH_3)_3$ is built and attached to the N7 position of each desired guanine via a Pt−N7 bond. An energy minimization calculation is run for 100 iterations to allow the Pt coordination sphere to form its desired bond lengths and angles. The linker group is then attached to complete the structure. This is done by placing the pre-minimized BBR3464 molecule at the desired position (either inside or outside the major groove), deleting the two $Pt(NH_3)_2Cl$ groups of the BBR3464, deleting the NH_3 groups trans to the N7 groups, and creating a bond between the Pt bound to the guanine and the now terminal NH_2 groups of the linker. Charges for BBR3464 were defined using an empirical charge distribution method. The +2 charge of each platinum was distributed so that charges corresponding to calculated values for ammine/amine nitrogens and hydrogens were assigned. Minimization was then performed using a conjugate gradient algorithm to a convergence criterion of 0.0418 kJ/mol (*21*).

Immunochemical Analysis. Polyclonal antibodies, Ab_{cis} and Ab_{trans}, were prepared against double-helical calf thymus DNA modified by cisplatin or transplatin, respectively, at r_b

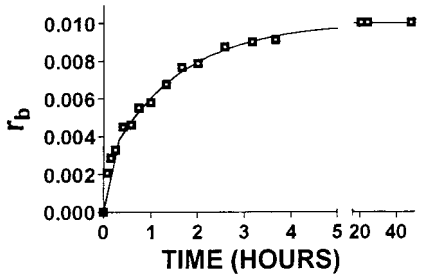

FIGURE 2: Kinetics of the binding of BBR3464 (□) to calf thymus DNA in the medium of 10 mM $NaClO_4$ at 37 °C determined by differential pulse polarographic assay. The concentration of DNA was 32 μg/mL, and r_i was 0.01.

= 0.08 in 10 mM $NaClO_4$ for 48 h at 37 °C. They were purified and characterized in the same way as described in previously published papers (*22*−*24*). Their specificity and avidity were the same as described in previous reports. The procedures for their immunoenzymatic analysis and ELISA have been also described (*22*−*24*).

RESULTS AND DISCUSSION

Physical Measurements. DNA Binding. Solutions of calf thymus DNA at a concentration of 0.32 mg/mL were incubated with BBR3464 at r_i values of 0.01 in 10 mM $NaClO_4$ at 37 °C (r_i is defined as the molar ratio of free platinum complex to nucleotide phosphates at the onset of incubation with DNA). At various time intervals an aliquot of the reaction mixture was withdrawn and assayed by DPP for platinum not bound to DNA. The amount of platinum bound to DNA (r_b) was calculated by subtracting the amount of free (unbound) platinum from the total amount of platinum present in the reaction. No changes in the pH of the reaction mixture containing DNA and BBR3464 were measured within 48 h after mixing DNA with the platinum complex. The amount of platinum coordinated to DNA increased with time, and after approximately 6 h, the complex was quantitatively bound (Figure 2). The half-time ($t_{1/2}$) of this binding reaction was ∼40 min. The binding of the trinuclear platinum complex is considerably faster than that of the dinuclear complex BBR3005 or cisplatin under similar conditions ($t_{1/2}$ ∼200−300 min or 4 h, respectively; ref *25*, Table 1). In a further experiment, a 2 h incubation on calf thymus DNA showed the relative molar amounts of Pt bound to be 7.3:1.8:1 for BBR3464 (+4 charge), BBR3005 (+2), and cisplatin, respectively (data not shown).

The rapid and essentially quantitative binding of BBR3464 facilitates sample analysis. The binding experiments (Figure 2) indicate that such platination reactions resulted in the coordination of all molecules of the platinum complexes, making it possible to prepare easily and precisely DNA samples modified at a preselected value of r_b. The samples of modified DNA which were further analyzed in this work by biochemical or biophysical techniques have been prepared by incubating DNA with the platinum complexes for 48 h except where stated (see also the Materials and Methods section).

DNA Melting. Calf thymus DNA was modified by BBR3464 to various r_b values (0−0.05) in 10 mM $NaClO_4$ at 37 °C for 48 h. Salt concentration was then further adjusted by the addition of $NaClO_4$ to the values in the range 0.01−0.2 M. The effect on t_m is dependent both on the amount of platinum bound and the salt concentration. At low concentrations of $NaClO_4$ (0.01 M) an increase of t_m is observed even at relatively high levels of the modification of DNA by BBR3464 (r_b = 0.05). At high salt concentrations of 0.1−0.2 M the modification of DNA by BBR3464 resulted in a *decrease* of t_m which became more pronounced with increasing r_b values (Figure 3C). This behavior is in marked contrast to cisplatin, where the modification of DNA results in a decrease of t_m if DNA melting is measured in salt concentrations from 0.01 to 0.2 M (Figure 3A). The dinuclear compound BBR3005 represents an intermediate case, with an increase in t_m at low ionic strength and relatively little change at the higher salt values. The latter effect is independent of the r_b value (Figure 3C and ref *25*).

Table 1: Summary of DNA Binding of Trinuclear BBR3464 and Comparison with DNA Binding of Dinuclear BBR3005 and Mononuclear Cisplatin

	BBR3464 (1,0,1/t,t,t)	BBR3005 (1,1/t,t n=6)	cisplatin
DNA binding ($t_{1/2}$) (min)	40[a]	200−300[b]	∼240[c]
sequence preference	G, GG[a]	G, GG, A[b]	GG, AG[c,d]
decrease of EtBr fluorescence	strong[a]	strong[a]	medium[a]
% interstrand cross-links/ adduct (after 48 h)	20[a]	70−90[b]	6[e]
unwinding angle/adduct	14°[a]	10−14°[f,g]	13°[f,h]
melting temperature			
high ionic strength	decrease[a]	no change[b]	decrease[i]
low ionic strength	increase[a]	increase[b]	decrease[i]
inhibition of antibodies			
Ab_{cis}	no[a]	no[b]	yes[a]
Ab_{trans}	yes[a]	yes[b]	no[a]

[a] This work. [b] Žaludová et al. (1997) *Eur. J. Biochem. 246*, 508. [c] Bancroft et al. (1990) *J. Am. Chem. Soc. 112*, 6860. [d] Eastman (1987) *Pharmacol. Ther. 34*, 155. [e] Lemaire et al. (1991) *Proc. Natl. Acad. Sci. U.S.A. 88*, 1982. [f] Keck and Lippard (1992) *J. Am. Chem. Soc. 114*, 3386. [g] Farrell et al. (1995) *Biochemistry 34*, 15480. [h] Bellon et al. (1991) *Biochemistry 30*, 8026. [i] Žaludová et al. (1997) *Biophys. Chem. 60*, 135. [j] Brabec et al. (1990) *Biophys. Chem. 35*, 129.

Previously, three factors have been invoked to account for the thermal stability of DNA modified by platinum(II) complexes: stabilizing effects of the positive charge on the platinum(II) moiety and of DNA interstrand cross-links, and a destabilizing effect of conformational distortions such as intrastrand cross-links induced in DNA by platinum coordination (*26*). The dependence of transition melting temperature on ionic strength was explained by competing electrostatic effects as salt concentration was varied. Under the incubation conditions, we expect all bifunctional platinum compounds to have produced a range of inter- or intra-strand cross-links. The observed change in melting temperature will reflect the relative proportion and contribution of the two limiting binding modes. Inherently, we predict intrastrand cross-linking to destabilize the helix, as has been consistently observed in studies with cisplatin. In contrast, interstrand cross-linking is predicted to stabilize the helix by preventing strand dissociation. However, it cannot be excluded that conformational distortions of novel interstrand cross-links could also result in destabilization of the helix. At low ionic strength, it is reasonable to conclude that the increases in t_m are caused by the high percentage of interstrand cross-links formed by both the dinuclear and trinuclear compound and by positive charges on platinum moieties. An interesting and as yet unresolved question, therefore, is why high salt appears to result in destabilization, even in the presence of interstrand

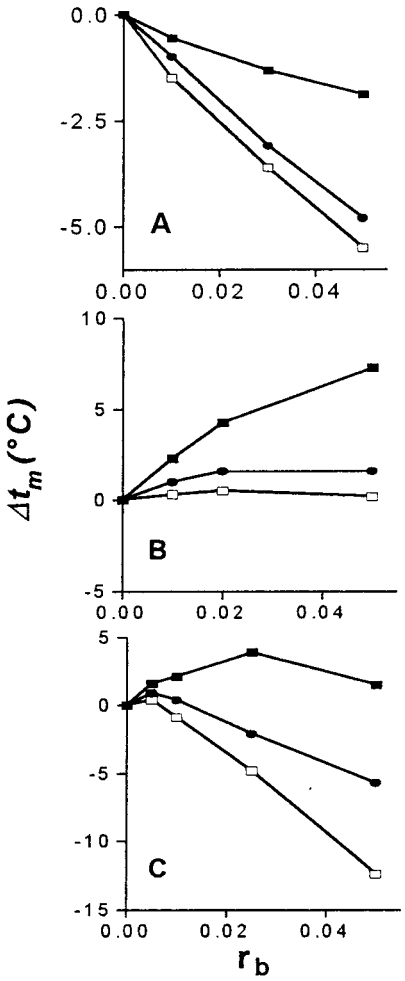

FIGURE 3: Plots of Δt_m values of calf thymus DNA modified by cisplatin (A), BBR3005 (B), or BBR3464 (C) on r_b. The t_m values were measured in media containing 0.01M (■), 0.1 M (●), or 0.2 M (□) $NaClO_4$; the solutions also contained 1 mM Tris-HCl and 0.1 mM EDTA, pH 7.4 (Δt_m is defined as the difference between the t_m values of platinated and nonmodified DNAs).

cross-links. It is possible that the observed decrease in t_m at high ionic strength is a consequence of conformational changes induced by the platinum adducts that then dominate over the combination of "stabilizing" effects. At high salt concentration the stabilizing effects are reduced since electrostatic effects of the platinum compounds are apparently lowered with increasing concentrations of Na^+ counterions. Thus, the solution behavior of the DNA adducts of BBR3464 appears significantly different from that of cisplatin and merits further study.

Characterization of DNA Adducts by EtBr Fluorescence. EtBr as a fluorescent probe has been used to characterize perturbations induced in DNA by bifunctional adducts of several mononuclear platinum compounds (*13*, *14*, *27*, *28*). Double-helical DNA was first modified by cisplatin, monofunctional [PtCl(dien)]Cl, dinuclear BBR3005, or trinuclear BBR3464 for 48 h. The levels of the modification corresponded to the values of r_b in the range between 0 and 0.1. Modification of DNA by all platinum complexes resulted in a decrease of EtBr fluorescence (Figure 4). The decrease caused by the adducts of dinuclear and trinuclear platinum complexes was similar and markedly more pronounced than that induced by the DNA adducts of cisplatin at equivalent r_b values. Modification of DNA by monofunctional platinum

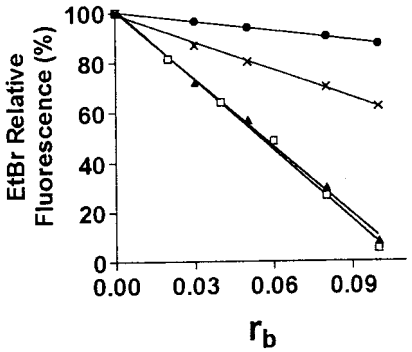

FIGURE 4: Dependences of the EtBr fluorescence on r_b for DNA modified by various platinum complexes in 10 mM $NaClO_4$ at 37 °C for 48 h: (●) [PtCl(dien)]Cl, (×) cisplatin, (▲) BBR3005, (□) BBR3464.

complexes results in only a slight decrease of EtBr fluorescence intensity as compared with the control DNA−EtBr complex (*13*, *14*, *27*, *28*). The structures of dinuclear and trinuclear DNA adducts arise from two monofunctional substitutions on the polynucleotide. Comparison with [PtCl(dien)]Cl suggests that the conformational distortion induced in DNA by these adducts is much more delocalized and extends over considerably more base pairs around the platination sites than in the case of the adducts of mononuclear complexes such as cisplatin or transplatin. Thus, these results are consistent with the formation of long-range intra- or interstrand cross-links of dinuclear and trinuclear platinum complexes.

Interstrand Cross-Linking. Long-range cross-links can readily occur in DNA because of the distance between reactive sites: the Pt−Pt distance in BBR3464 is 0.229 nm from the crystal structure and 0.253 nm from the model. The principal reason for this discrepancy is that the crystal structure shows a slight "curvature" of the molecule possibly because of packing interactions, whereas the model produces an essentially linear array of the three Pt coordination spheres. Taking into account the approximate 0.021 nm distance of a standard Pt−N (purine) bond, it is clear that the BBR3464 molecule can easily span 6−8 base pairs. The calculated Pt−Pt distance of 0.12 nm for BBR3005 is consistent with the ability to form at least 1,4 cross-links (*29*). Finally, the preponderance of 1,2 cross-links induced by cisplatin is also fully understandable in light of the 0.034 nm separation of the two neighboring Cl ligands.

An expected result, then, for BBR3464 is that DNA−DNA interstrand cross-linking will occur. For quantitation of this feature, pSP73 plasmid (2464 bp) was linearized by *Eco*RI (*Eco*RI cuts only once within pSP73 plasmid) and modified by the trinuclear platinum complex at various r_b values. The samples were analyzed for the interstrand cross-links by agarose gel electrophoresis under denaturing conditions (*15*). Upon electrophoresis under denaturing conditions, 3′-end-labeled strands of linearized pSP73 plasmid containing no interstrand cross-links migrate as a 2464-base single strand, whereas the interstrand cross-linked strands migrate more slowly as a higher molecular mass species. The bands corresponding to more slowly migrating interstrand *cross*-linked fragments were seen for r_b values as low as 1×10^{-4} (Figure 5A, lane 2). The intensity of the more slowly migrating band increased with the growing level of the modification. The radioactivity associated with the individual

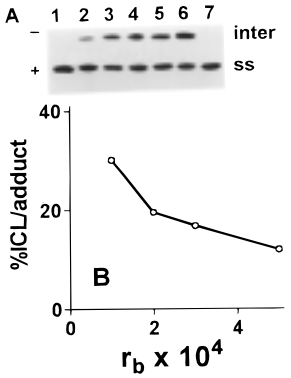

FIGURE 5: The formation of interstrand cross-links by BBR3464 in linearized pSP73 plasmid (2464 bp). (A) Autoradiogram of denaturing 1% agarose gels of linearized DNA which was 3′-end-labeled. The interstrand cross-linked DNA appears as the top bands migrating on the gel more slowly than the single-stranded DNA (contained in the bottom bands). Plasmid linearized by *Eco*RI was incubated for 48 h with BBR3464 at r_b values of 0 (control) (lanes 1 and 7 in panel A), 1×10^{-4}, 2×10^{-4}, 3×10^{-4}, 5×10^{-4}, and 7×10^{-4} (lanes 2−6 in panel A, respectively). (B) Dependence on r_b of the number of interstrand cross-links per adduct (percent of interstrand cross-link per adduct) formed by BBR3464 in linearized DNA after 48 h. The ratio of interstrand cross-links to the complex bound was calculated as described previously (*4*, *15*). The percent of interstrand cross-link per adduct (%ICL/adduct) was then calculated by multiplying this ratio by 100.

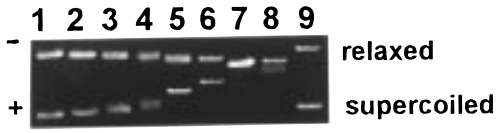

FIGURE 6: Unwinding of supercoiled pSP73 plasmid DNA by BBR3464. The top bands correspond to the form of nicked plasmid and the bottom bands to closed, negatively supercoiled plasmid. The plasmid was incubated with BBR3464 with the r_b values of 0 (control) (lanes 1 and 9), 0.001, 0.005, 0.01, 0.02, 0.03, 0.04, and 0.05 (lanes 2−8, respectively).

bands in each lane was measured to obtain estimates of the fraction of non-cross-linked or cross-linked DNA under each condition. The frequency of interstrand cross-links was calculated using the Poisson distribution from the fraction of non-cross-linked DNA in combination with the r_b values and the fragment size. The interstrand cross-link frequency decreased slightly with growing r_b values. For instance, at $r_b = 2 \times 10^{-4}$, ~20% molecules of linearized DNA were cross-linked due to the modification by BBR3464 (Figure 5B). Thus, the DNA interstrand cross-linking efficiency of BBR3464 was significantly higher than that of cisplatin (6%; ref *15*), but markedly lower than that of the diamine-linked dinuclear complexes such as BBR3005 (70−90%; ref *25*). An interesting consequence of increasing length and/or charge therefore is that the discrimination between interstrand and intrastrand cross-linking is diminished.

Unwinding Induced in DNA by the Binding of Trinuclear Platinum Complexes. Electrophoresis in native agarose gel was used to quantify the unwinding induced in pSP73 plasmid by the platinum complexes by monitoring the degree of supercoiling (Figure 6). A compound that unwinds the DNA duplex reduces the number of supercoils so that the superhelical density of closed circular DNA decreases. This decrease upon binding of unwinding agents causes a decrease in the rate of migration through agarose gel, which makes it possible that the unwinding can be observed and quantified. Figure 6 shows an electrophoresis gel in which increasing amounts of BBR3464 have been bound to a mixture of relaxed and supercoiled pSP73 DNA. Interestingly, the trinuclear complex accelerated the mobility of the relaxed form in a way similar to that of cisplatin, whose bifunctional binding to DNA shortens and condenses the DNA helix (*30*, *31*). The unwinding angle is given by $\Phi = 18\sigma/r_b(c)$ where σ is the superhelical density and $r_b(c)$ is the value of r_b at which the supercoiled and relaxed forms comigrate (*16*). Under the present experimental conditions, σ was calculated to be −0.063 on the basis of the data of cisplatin for which the $r_b(c)$ was determined in this study and $\Phi = 13°$ was assumed. By using this approach, we determined the DNA unwinding angle of 14° ± 1° for BBR3464.

The values of unwinding angles are affected by the nature of the ligands in the coordination sphere of platinum and the stereochemistry at the platinum center. A previous systematic work revealed that the platinum(II) compounds fall into different classes according to their DNA-binding modes (*16*). It has been shown that platinum(II) compounds with the smallest unwinding angles (6°) are those that can bind DNA only monofunctionally {[PtCl(dien)]Cl or [PtCl-$(NH_3)_3$]Cl}. Another group of platinum compounds is composed of those which bind to DNA in a bifunctional manner. The compounds which belong to this category unwind DNA by 10°−13° and include cisplatin, its trans isomer, and bifunctional dinuclear complexes such as BBR3005 (*5*). The observation that BBR3464 can be grouped with other bifunctional platinum(II) compounds is readily understood in terms of adduct structures in which the complex is preferentially coordinated to DNA in a bifunctional manner.

Sequence Preference of DNA Adducts. The rapid binding to DNA and the effect of charge may affect sequence specificity of an agent such as BBR3464. This procedure involved the extension by $Vent_R(exo^+)$ DNA polymerase at the 3′-end of the 5′-end radioactively labeled primer up to the metal adduct on the template strand of pSP73 plasmid. By using thermal cycling, we repeated this process many times in order to amplify the signal. The products of this linear amplification were then examined on DNA sequencing gels, and the sequence specificity of the platinum adduct formation was determined to the exact base pair. $Vent_R(exo^+)$ DNA polymerase has 3′ → 5′ exonuclease activity, similar to that of several other native DNA polymerases. For mapping studies to detect the location of metal−DNA adducts in a heterogeneous population, DNA polymerases, which have active 3′ → 5′ exonuclease, are suitable.

In vitro DNA synthesis on double-stranded templates containing the adducts of BBR3464 generated a population of DNA fragments, indicating that these adducts terminate duplex synthesis (Figure 7A, lane triPt). If the same synthesis was performed with $Vent_R(exo^-)$ DNA polymerase [genetically engineered from $Vent_R(exo^+)$ DNA polymerase and retaining the polymerase activity but having no 3′ → 5′ exonuclease activity], the sequence dependence of the termination was considerably less regular (not shown). Sequence analysis of the termination sites produced by the trinuclear platinum complex suggests a strong sequence preference for single dG sites or d(GG) sequence in double-helical DNA (Figure 7B). In agreement with the *in vitro*

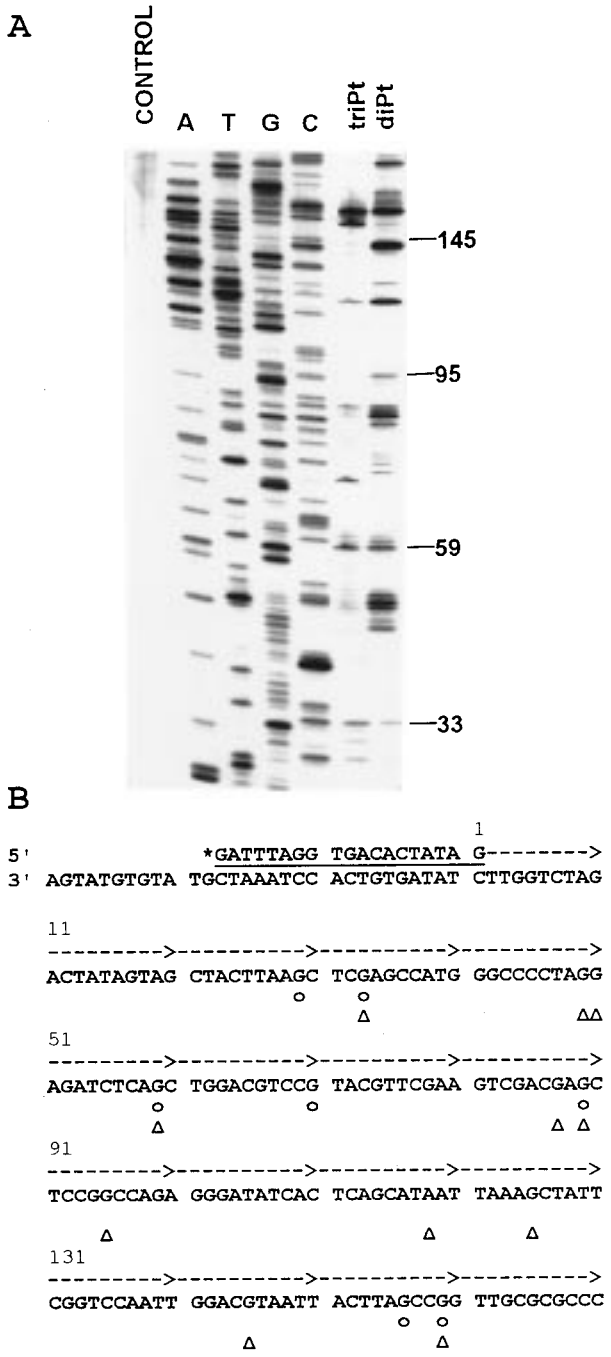

FIGURE 7: (A) Autoradiogram of 6% polyacrylamide/8 M urea sequencing gel showing inhibition of DNA synthesis by $Vent_R$ DNA polymerase on the pSP73 plasmid DNA linearized by *Nde*I restriction enzyme and subsequently modified by bifunctional dinuclear or trinuclear platinum complexes. The gel contained the linear amplification products of control, nonplatinated DNA, and DNA treated with BBR3464 or BBR3005 complexes. Lanes: control, unmodified template; A, T, G, C, chain-terminated marker DNAs (note that these dideoxy sequencing lanes give the sequence complementary to the template strand); triPt, DNA modified by BBR3464 at $r_b = 0.005$; and diPt, DNA modified by BBR3005 at $r_b = 0.005$. The numbers correspond to the nucleotide sequence numbering of panel B. (B) Schematic diagram showing a portion of the sequence used to monitor inhibition of DNA synthesis on the template containing adducts of the BBR3464 or BBR3005 complexes. The star indicates the 5′-end labeling of the primer (its nucleotide sequence is underlined). The arrow indicates the direction of the synthesis: ○, major stop signals from panel A, lane triPt; and △, major stop signals from panel A, lane diPt. The numbering of the nucleotides in this scheme corresponds to the numbering of the nucleotides in the pSP73 nucleotide sequence map.

transcription mapping of DNA adducts of BBR3005 (1,1/t,t $n = 6$) published recently (*25*), this complex also exhibited a strong preference for single dG sites or d(GG) sequences (Figure 7A, lane diPt). However, BBR3005 formed more blocks on DNA for DNA−polymerase than the trinuclear complex and most of them at different sequences. In addition, this mapping also revealed a strong termination site in the sequence d(AAT) at its central dA site [position 118 in the nucleotide sequence map of pSP73 plasmid (Figure 7B)]. This is not a known DNA-binding site for platinum complexes, confirming less regular sequence specificity of BBR3005 in comparison with BBR3464. The high DNA affinity and rapid binding of BBR3464 may be responsible for its enhanced sequence specificity.

Molecular Modeling of DNA Adducts of BBR3464. The conformational changes on DNA induced by BBR3464 show some similarities to BBR3005, and both patterns are very distinct from that of cisplatin. To summarize, unwinding experiments confirm bifunctional binding but interstrand cross-linking is lower than might be expected, while still significantly higher than that of cisplatin. Thus, the remainder of the adducts are likely to be long-range intrastrand. The efficiency of inhibition of EtBr fluorescence is in agreement with high occupancy over extended regions.

The sequencing studies (Figure 7) indicate that high charge and high DNA affinity result in enhanced sequence specificity for BBR3464. For small molecules such as cisplatin, it is easy to use sequencing studies to deduce the structural nature of the adduct, as the lesion does not extend over many base pairs. An inherently interesting problem in deducing the nature of stop sites caused by BBR3464 adducts (and indeed all dinuclear and trinuclear long-range cross-linking agents) is that it is difficult to predict exactly where the other end of the molecule is located. A novel assay has been employed to assign sites of interstrand cross-linking of 1,1/t,t $n = 4$ (*29*). In the present study, molecular modeling was used to gain information about the DNA structural changes induced by drug binding.

Consider the following sequence:

5′– T'_{23} G'_{24} A'_{25} A'_{26} T'_{27} T'_{28} C'_{29} G'_{30} A'_{31} G'_{32} C'_{33} T'_{34} C'_{35} G'_{36} G'_{37} T'_{38} A'_{39}

3′– A_{23} C_{24} T_{25} T_{26} A_{27} A_{28} G_{29} C_{30} T_{31} C_{32} G_{33} A_{34} G_{35} C_{36} C_{37} A_{38} T_{39}

This sequence corresponds to a 17-base pair fragment beginning with T'_{23} in the top strand of the original sequence of pSP73 DNA from the 5′-end (Figure 7B). Within this sequence two stop sites were observed corresponding to G_{29} and G_{33} of the bottom strand of the original plasmid (Figure 7B). If we consider initial monofunctional binding to G_{33} a number of adducts are possible, taking into account only guanine binding in the second bifunctional step. Since dinuclear and trinuclear platinum compounds are expected to exhibit binding specificity in the 5′ → 5′ direction for interstrand cross-linking (ref *29* and Kašpárková et al., unpublished experiments), a 1,4 interstrand cross-link could occur between G_{33} and G'_{30}. A 1,5 intrastrand cross-link from the same G_{33} site to G_{29} is also possible**.** These two adducts would explain the two stop sites observed. Molecular modeling was performed to calculate a relative energy for these two species. There were two models of the 1,4 interstrand cross-link, differing only in the position of the linker group. This relatively short cross-link allows for more

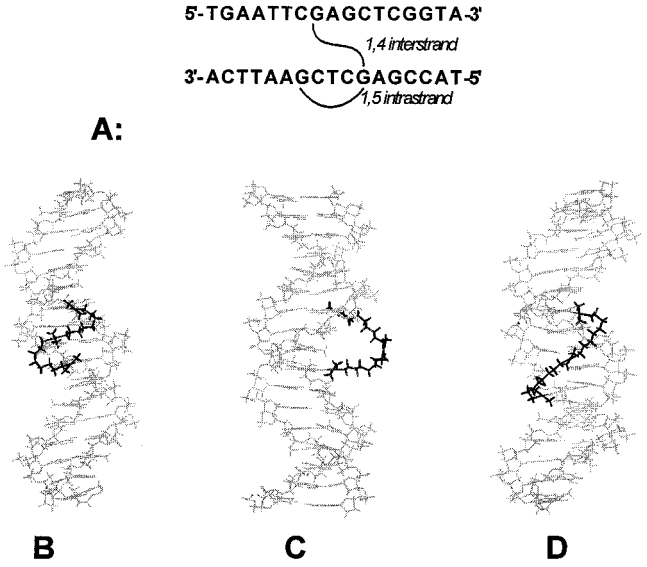

FIGURE 8: Structural representation of adducts formed by BBR3464 on double-stranded DNA in the sequence 5′-d(TGAATTCGAGCTCGGTA)/5′-d(TACCGAGCTCGAATTCA). (A) Schematic of the cross-links. (B) The 1,4 interstrand cross-link, with the linker positioned within the major groove (−2751.4 kJ/mol). (C) The 1,4 interstrand cross-link, with the linker positioned outside of the major groove (−2751.8 kJ/mol). (D) The 1,5 intrastrand cross-link (−2894.1 kJ/mol).

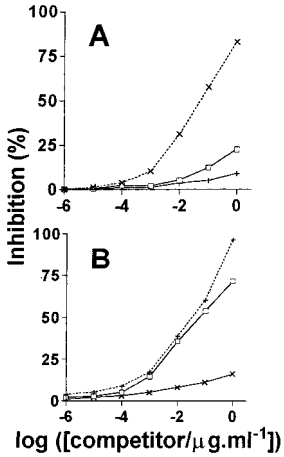

FIGURE 9: Competitive inhibition in an ELISA of the binding of the antibodies elicited against double-helical DNA modified by cisplatin (Ab_{cis}) (A) or transplatin (Ab_{trans}) (B) to the competitor which was double-helical DNA platinated at $r_b = 0.02$. The competitor was double-helical DNA modified by cisplatin (×), BBR3464 (□), or transplatin (+). The inhibition expresses the antibody binding as a percentage of binding in the absence of any competitor. Data points measured in triplicate varied on average by ±2% from their mean.

conformational flexibility in the linker. Therefore, the following models for two linker positions for this shorter cross-link are proposed: (1) with the linker positioned within the major groove, and (2) with the linker outside the major groove. The various cross-links modeled can be seen in Figure 8. An interesting feature is the total energy of each structure. The energy of the 1,5 intrastrand cross-link is relatively the lowest (−2894.1 kJ/mol). The major contribution to the lower energy is from decreased dihedral strain and van der Waals energies. The low strain energy is due to the relaxed position (extended) of the linker group relative to the shorter 1,4 interstrand cross-link structures. The total energy of the 1,4 interstrand cross-link with linker outside the major groove is −2751.8 kJ/mol. The 1,4 interstrand cross-link with linker inside the major groove has an energy of −2751.4 kJ/mol. The similarity in energies is attributed to strain being present in different sections of each model. The model with the linker group within the groove exhibits strain in the BBR3464 molecule, while the model with the linker outside the major groove exhibits DNA strain in the region of platinum binding. The use of molecular mechanics alone is limiting in the attempt to predict the structure of a system and its components. However, it is a very useful tool to obtain more information on the structure to attempt to explain the physical results. These initial modeling calculations indicate that long-range intrastrand and interstrand cross-links are almost equally favored. Whether this is due to the chain length of BBR3464 being so flexible or the charge along the backbone is yet to be determined.

Immunochemical Analysis. The premise of this drug development effort was that compounds structurally dissimilar to cisplatin would, by virtue of a different spectrum of DNA binding, produce antitumor effects different from those of cisplatin (*3*). An important aspect for any new drug, therefore, is whether its DNA adducts will be recognized by antibodies raised to cisplatin. To answer this question, we have prepared two types of antibodies, one of which binds specifically to DNA modified by cisplatin and its direct structural analogues (Ab_{cis}), while the other binds specifically to DNA modified by transplatin (Ab_{trans}). Ab_{cis} recognized two neighboring purine residues of the same strand of DNA cis coordinated to the platinum atom of *cis*-$[Pt(amine)_2]^{2+}$ moiety (*22*, *24*). On the other hand, Ab_{trans} recognized specifically a short single-stranded segment in double-stranded DNA containing the platinated site; this platinated site was either an intrastrand cross-link between two nonadjacent base residues in DNA trans coordinated to the platinum atom of *trans*-$[Pt(amine)_2]^{2+}$ moiety or the platinum(II) atom coordinated in only a monofunctional manner (*23*).

By using competitive ELISA, we measured the inhibition of the binding of Ab_{cis} or Ab_{trans} to their immunogens (double-stranded calf thymus DNA modified by cisplatin or transplatin at $r_b = 0.08$ for 48 h, respectively) by double-stranded DNA modified by BBR3464 at various r_b values in the range 0.005−0.1. Double-stranded DNA modified by BBR3464 did not inhibit the binding of the Ab_{cis} (shown for $r_b = 0.02$ in Figure 9A). In contrast, DNA modified by BBR3464 inhibited the binding of the Ab_{trans} to their immunogen with an efficiency similar to that of DNA modified by transplatin (shown for $r_b = 0.02$ in Figure 9B) or by dinuclear complexes such as BBR3005 under identical conditions (*25*). The observation that DNA modified by the trinuclear platinum complex did not inhibit Ab_{cis} is easily understood to reflect the fact that no DNA adducts of the trinuclear platinum complex produce conformational transitions similar to those of cisplatin. In contrast, the good recognition of DNA modified by BBR3464 by Ab_{trans} (Figure 9B) suggests that this modification has features recognized by these antibodies similar to those which appear in DNA after its modification by transplatin. There may be a subset of adducts which are recognized as "purely" monofunctional if there is

no long-range conformational change. Thus, the bifunctional DNA adducts of trinuclear BBR3464 could have some structural features similar to monofunctional platinum(II) adducts.

CONCLUSIONS

The biochemical and biophysical analysis of DNA interactions with the bifunctional trinuclear platinum(II) anticancer drug, BBR3464 (1,0,1/t,t,t), described in this report and summarized in Table 1 provides experimental support that the binding of this platinum complex modifies DNA in a way which is different from that by cisplatin. As DNA is a main pharmacological target of platinum(II) complexes, the latter view is also consistent with the hypothesis that the radically altered DNA-binding mode of BBR3464 is a very important factor responsible for altered cytostatic activity of this new trinuclear platinum complex in tumor cells (in comparison with cisplatin). The rapid binding of BBR3464 caused by the high charge results in enhanced sequence specificity. An intriguing aspect of BBR3464 is that, in adding charge and increasing chain length, interstrand cross-linking is diminished relative to BBR3005 and long-range intrastrand cross-links become equally probable! These types of lesions have critical consequences for the biological functions of DNA; the resulting conformational alterations in DNA may play an important role in considerably altered antitumor effects of this new platinum complex as compared with cisplatin. Thus, "downstream" effects modulated by protein recognition and binding are not likely to be the same as the subset of proteins which recognize cisplatin (*32*). In agreement with this point, antibodies raised to cisplatin do not recognize the adducts formed by BBR3464.

The results also indicate that BBR3005 and BBR3464 share a general profile. The enhanced antitumor activity of BBR3464 may therefore be assigned to the effects due to the increase in charge. The designed synthesis of *dinuclear* platinum complexes with hydrogen-bonding ligands such as spermine (total charge +4) and spermidine (total charge +3) linkers mimics the essential biological features of BBR3464 (*6*, *33*). Thus, increased charge enhances antitumor activity, at least within the polynuclear platinum family. To explain fully the antitumor activity of BBR3464, one should also take into account pharmacological factors. In both human osteosarcoma (*34*) and murine leukemia (Roberts et al., 1999, unpublished results) cell lines, BBR3464 accumulation and DNA binding are much higher than for cisplatin. The fact that a +4 compound shows *enhanced* cellular accumulation in comparison to the neutral cisplatin is a unique and totally unexpected finding from the classical structure−activity relationships of platinum complexes. However, DNA binding at equitoxic concentrations was similar, indicating that the BBR3464 adducts were more effective at cell killing. Measurement of *intracellular* interstrand cross-linking in both of these cell lines confirmed that the interstrand cross-link is formed, but is not a major component. The time course of interstrand cross-link formation and removal is different to that of cisplatin, confirming their structural differences. Thus, either the interstrand cross-links are exceptionally potent or the cytotoxicity of BBR3464 must be considered as a sum of all of the possible lesions. The evidence from this work that the overall profile of long-range intra- and interstrand cross-links produces delocalized lesions on DNA may explain the effectiveness. In summary, the chemical and biological features outlined here argue that the drug should be considered the first clinical representative of an entirely new structural class of DNA-modifying anticancer agents.

REFERENCES

1. Farrell, N. P., De Almeida, S. G., and Skov, K. A. (1988) *J. Am. Chem. Soc. 110*, 5018−5019.
2. Qu, Y., Appleton, T. G., Hoeschele, J. D., and Farrell, N. (1993) *Inorg. Chem. 32*, 2591−2593.
3. Farrell, N. (1996) in *Advances in DNA Sequence Specific Agents* (Hurley, L. H., and Chaires, J. B., Eds.) JAI Press Inc., New Haven, CT pp 187−216.
4. Farrell, N., Qu, Y., Feng, L., and Van Houten, B. (1990) *Biochemistry 29*, 9522−9531.
5. Farrell, N., Appleton, T. G., Qu, Y., Roberts, J. D., Fontes, A. P. S., Skov, K. A., Wu, P., and Zou, Y. (1995) *Biochemistry 34*, 15480−15486.
6. Farrell, N., Qu, Y., Bierbach, U., Valsecchi, M., and Menta, E. (1999) in *30 Years of Cisplatin - Chemistry and Biochemistry of a leading Anticancer Drug* (Lippert, B., Ed.) Verlag CH, Basel, Switzerland pp 479−496.
7. Farrell, N., and Spinelli, S. (1998) in *Uses of Inorganic Chemistry in Medicine* (Farrell, N., Ed.) Royal Society of Chemistry, Cambridge, U.K. (in press).
8. Ruley, H. E. (1997) in *Principles and Practice of Gynecological Oncology Updates*, pp 1−19, Lippincott-Raven Healthcare, Cedar Knotts, NJ.
9. Qu, Y., and Farrell, N. (1992) *Inorg. Chem. 31*, 930−932.
10. Brabec, V., and Paleèek, E. (1970) *Biophysik (Berlin) 6*, 290−300.
11. Brabec, V., and Paleèek, E. (1976) *Biophys. Chem. 4*, 76−92.
12. Kim, S. D., Vrána, O., Kleinwächter, V., Niki, K., and Brabec, V. (1990) *Anal. Lett. 23*, 1505−1518.
13. Butour, J. L., and Macquet, J. P. (1977) *Eur. J. Biochem. 78*, 455−463.
14. Butour, J. L., Alvinerie, P., Souchard, J. P., Colson, P., Houssier, C., and Johnson, N. P. (1991) *Eur. J. Biochem. 202*, 975−980.
15. Brabec, V., and Leng, M. (1993) *Proc. Natl. Acad. Sci. U.S.A. 90*, 5345−5349.
16. Keck, M. V., and Lippard, S. J. (1992) *J. Am. Chem. Soc. 114*, 3386−3390.
17. Lemaire, M. A., Schwartz, A., Rahmouni, A. R., and Leng, M. (1991) *Proc. Natl. Acad. Sci. U.S.A. 88*, 1982−1985.
18. Nováková, O., Kašpárková, J., Vrána, O., vanVliet, P. M., Reedijk, J., and Brabec, V. (1995) *Biochemistry 34*, 12369−12378.
19. Yao, S., Plastaras, J. P., and Marzilli, L. G. (1994) *Inorg. Chem. 33*, 6061−6077.
20. Orozco, M., Laughton, C. A., Herzyk, P., and Neidle, S. (1990) *J. Biomol. Struct. Dyn. 8*, 359−373.
21. Qu, Y., Bloemink, M. J., Reedijk, J., Hambley, T. W., and Farrell, N. (1996) *J. Am. Chem. Soc. 118*, 9307−9313.
22. Lippard, S. J., Ushay, H. M., Merkel, C. M., and Poirier, M. C. (1983) *Biochemistry 22*, 5165−5168.
23. Brabec, V., Vrána, O., Kiseleva, V. I., and Poverenny, A. M. (1991) *Eur. J. Biochem. 201*, 723−730.
24. Vrána, O., Kiseleva, V. I., Poverenny, A. M., and Brabec, V. (1992) *Eur. J. Pharmacol. 226*, 5−13.
25. Žaludová, R., Žákovská, A., Kašpárková, J., Balcarová, Z., Kleinwächter, V., Vrána, O., Farrell, N., and Brabec, V. (1997) *Eur. J. Biochem. 246*, 508−517.
26. Žaludová, R., Kleinwächter, V., and Brabec, V. (1996) *Biophys. Chem. 60*, 135−142.
27. Brabec, V., Vrána, O., Nováková, O., Kleinwächter, V., Intini, F. P., Coluccia, M., and Natile, G. (1996) *Nucleic Acids Res. 24*, 336−341.
28. Žákovská, A., Nováková, O., Balcarová, Z., Bierbach, U., Farrell, N., and Brabec, V. (1998) *Eur. J. Biochem. 254*, 547−557.

29. Zou, Y., Vanhouten, B., and Farrell, N. (1994) *Biochemistry 33*, 5404−5410.
30. Cohen, G. L., Bauer, W. R., Barton, J. K., and Lippard, S. J. (1979) *Science 203*, 1014−1016.
31. Scovell, W. M., and Collart, F. (1985) *Nucleic Acids Res. 13*, 2881−2895.
32. Zlatanova, J., Yaneva, J., and Leuba, S. H. (1998) *FASEB J. 12*, 791−799.
33. Rauter, H., Di Domenico, R., Menta, E., Oliva, A., Qu, Y., and Farrell, N. (1997) *Inorg. Chem. 36*, 9307−9313.
34. Perego, P., Caserini, C., Gatti, L., Carenini, N., Romanelli, S., Supino, R., Colangelo, D., Viano, I., Spinelli, S., Pezzoni, G., Manzotti, C., Farrell, N., and Zunino, F. (1999) *Mol. Pharmacol. 55*, 528−534.

BI990124S